Statistical mechanics of the two-dimensional hydrogen-bonding self-avoiding walk including solvent effects

D. P. Foster and C. Pinettes
Laboratoire de Physique Théorique et Modélisation (CNRS UMR 8089), Université de Cergy-Pontoise, 2 Avenue A. Chauvin 95302 Cergy-Pontoise Cedex, France
(Received 27 October 2007; published 15 February 2008)

A two-dimensional square-lattice model for the formation of secondary structures in proteins, the hydrogen-bonding model, is extended to include the effects of solvent quality. This is achieved by allowing configuration-dependent nearest-neighbor interactions. The phase diagram is presented and found to have a much richer variety of phases than either the pure hydrogen-bonding self-avoiding walk model or the standard Θ-point model.

DOI: 10.1103/PhysRevE.77.021115 PACS number(s): 05.40.Fb, 05.20.−y, 05.50.+q, 36.20.−r

I. INTRODUCTION

Self-avoiding walk models have been used for many years as models of real polymers in solution [1–3]. The thermodynamical behavior of a linear polymer in a good dilute solvent is dominated by its entropy, which may be well modeled by an excluded volume interaction, leading to the idealized model of a self-avoiding walk on a lattice. As the temperature of the polymer is lowered, typically the quality of the solvent is degraded, and the difference in affinity between the monomers (chemical building blocks of the polymer) and between the monomers and the solvent molecules becomes important. At low enough temperatures the polymer collapses and will precipitate from solution. This difference in affinities may be modeled in the self-avoiding walk model by an effective attractive interaction between neighboring steps of the walk. The high temperature (good solvent) and low temperature (bad solvent) regimes are separated by a phase transition point known as the Θ point.

The canonical model for this system is the Θ-point model, which consists of placing the interactions between nearest-neighbor lattice sites which have been visited nonconsecutively by the self-avoiding walk [4,5]. Typically this model is studied in the grand-canonical ensemble where the length of the walk is governed by a step fugacity K. The grand-canonical partition function $\mathcal{Z}$ is then written

$$\mathcal{Z} = \sum_{\text{walks}} K^N \tau^{N_I}, \tag{1}$$

where N is the length of the walk, N_I is the number of nearest-neighbor interactions, and $\tau = \exp(-\beta\epsilon)$, $\beta = 1/kT$, $\epsilon < 0$ is the (attractive) energy gained per nearest-neighbor contact. This model describes well the behavior of simple linear polymers in solution. The phase diagram in the fugacity and temperature plane is shown in Fig. 1. It is expected that any typical size of the walk, such as the radius of gyration, should scale as a power law with the length of the walk as follows:

$$R_G \sim \langle N \rangle^{\nu}, \tag{2}$$

where ν is simply the correlation length exponent defined in magnetic models. Indeed, the self-avoiding walk model may be mapped onto an $O(n)$ symmetric spin model in the limit $n \to 0$ [6]. It may then be seen that the phase transition line shown in Fig. 1 is the line on which the average length diverges, for large temperatures (small β) continuously and for low temperatures discontinuously. The Θ point is then identified with a tricritical point. While this model is of most practical importance in three dimensions, it has been extensively studied in two dimensions, because it is expected that the critical behavior is richer in two dimensions, particularly since the upper critical dimension of a tricritical point is 3.

An interesting question arises: the basic ingredients modeled by the Θ-point model which enable it to capture the essence of the real polymer in solution are the modeling of the entropic repulsion by the excluded volume interaction (self-avoidance) and the modeling of the short ranged attraction between the monomers. It should be expected, then, that any consistent way of modeling these two features would lead to a thermodynamically equivalent model. With this in mind, Blöte and Nienhuis [7] introduced a variant on the model in which the self-avoidance restriction is relaxed in that the walk can now visit lattice sites more than once, however, the walk is not allowed to visit the lattice bonds more than once, and the walk is not allowed to cross itself. The interactions are now introduced for the doubly visited

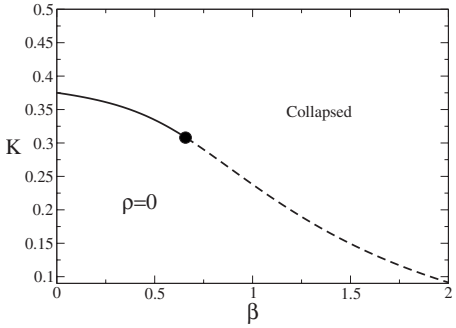

FIG. 1. The phase diagram for the standard Θ-point model, showing a low-K zero density (finite walk length) phase and a high-K (critical) collapsed phase, where the walk density is finite. At high temperatures (low β) the transition is second order (solid line), while at low temperatures (high β) the transition becomes first order (dashed line). These two behaviors are separated by a tricritical point, the Θ point.

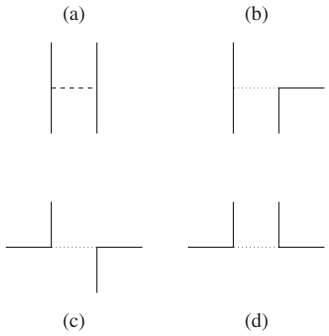

FIG. 2. The nearest-neighbor interactions are split into two classes, those of type (a) where four bonds forming two parallel lines model the hydrogen bonds, while the others [(b), (c) and (d)] model the solvent interactions. Configuration (a) induces a preferred orientation, while the other configurations do not.

sites. Surprisingly this model has a phase diagram which differs from the Θ-point model in many important respects: there is an extra phase transition in the dense region of the phase diagram. This phase line is in the Ising universality class with a value of the correlation length exponent $\nu=1$ [7,8]. The new collapse transition is not in the same universality class as the Θ point, having an exponent $\nu=12/23$ [9], as compared to $\nu=4/7$. At first sight these differences seem to be in contradiction with the idea of universality, which is required if we are even to think of modeling a polymer in solution by a lattice based walk model. In fact, universality is not violated. If the walk fills the lattice with a finite density, and its fractal (Haussdorf) dimension is the same as the lattice dimension, then the walk sees the lattice, and may be subject to lattice frustration effects. At the Θ point the density is zero, while it was shown that the density at the collapse transition in the Nienhuis-Blöte model is nonzero [10]. The presence of an Ising transition in the dense region is an indication that the lattice interactions tend to pick out a preferred direction, here corresponding to the lattice diagonals.

Other lattice models have been introduced which contain collapse transitions, notably the bond-interacting self-avoiding walk [11–13] and the hydrogen-bonding self-avoiding walk [14,15]. The first is simply the Θ point model in which the interactions are now between the nearest-neighbor visited lattice bonds. The Hydrogen-bonding self-avoiding walk was introduced to model the formation of secondary structures in proteins under the influence of the hydrogen bond. Hydrogen bonds are induced by dipole-dipole interactions, and impose an orientation on the interacting portions of the polymer. How these interactions are implemented in the Hydrogen model is shown in Fig. 2.

The bond-interacting self-avoiding walk has been studied using mean-field type calculations on the Bethe lattice [11] and the Husimi lattice [13]. These different studies have proposed radically different phase diagrams. A recent transfer matrix calculation [12] indicates that the correct phase diagram is that proposed by Buzano and Pretti [11], and shown schematically in Fig. 3. While there is a collapse transition in the same universality class as the standard Θ point, there is also the presence of an additional transition line in the dense region of the phase diagram. Unlike the Nienhuis-Blöte model, this transition line seems to be exotic in nature, with a nondivergent susceptibility [12].

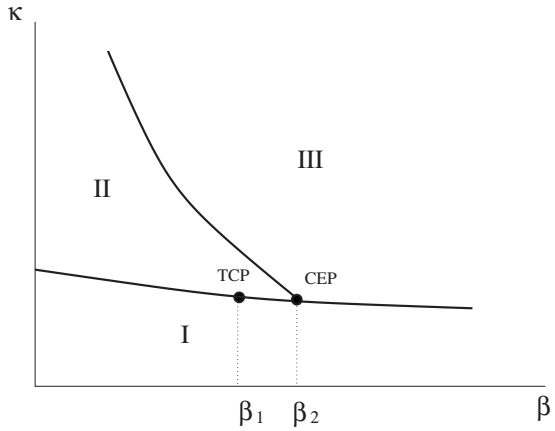

FIG. 3. A schematic version of the phase diagram for the bond-interacting self-avoiding walk model, proposed by Buzano and Pretti [11] and confirmed by Foster [12]. Phase I is the low-K finite walk phase, II is the critical collapsed (liquid) phase, and III is the crystalline oriented phase.

The hydrogen-bonding model was also investigated using transfer matrices [15]. The phase diagram was schematically similar to the Nienhuis-Blöte model, but the collapse transition was found to be first order. The high density transition line seemed not, in this study, to be in the Ising universality class, but the error bars were so large as to make it hard to rule out any possibility. We return to this question in this work, and using recently developed corner-transfer-matrix renormalization-group (CTMRG) methods [16] we manage to give an accurate estimate of the critical exponent ν, clearly ruling out any possibility that it could be in the Ising universality class.

Faced with this variety of different behaviors, it almost seems that any change to the model leads to different behavior for dense interacting self-avoiding walks. In order to investigate the relationship between these different behaviors we introduce an extension of the hydrogen-bonding self-avoiding walk model to include Θ-type interactions. These interactions are shown in Fig. 2. There is also a more direct motivation for these interactions; while a protein folds under the influence of the hydrogen bonds, it is still subject to the quality of the solvent. Indeed it is the quality of the solvent (or physiological temperature) which decides whether or not a protein is functional. We will show that this enlarged model contains several, if not all, of the different thermodynamic behaviors found above, and provides a unifying framework in which to understand the effect of geometrical frustration in lattice walk models.

In the next section the model is presented. In Sec. III results are first presented for two cases, showing two different behaviors. The results found then enable a mapping of the full phase diagram. The article ends with a discussion of the results.

II. THE MODEL

The model studied in this article involves the self-avoiding walk on the square lattice with interactions between

nonconsecutive visited nearest-neighbor sites on the lattice. Unlike the standard Θ-point model, the interactions are split into two sets, as shown in Fig. 2, between those which specify a particular direction, the hydrogen bonds, and those that do not, the solvent interactions. Hydrogen bonds carry an interaction energy $-\epsilon_H$ and the others carry an interaction energy $-\epsilon$. The thermodynamic behavior may be investigated by introducing the grand-canonical partition function $\mathcal{Z}$ from which many of the relevant thermodynamic quantities may be calculated. The grand-canonical partition function is given by

$$\mathcal{Z} = \sum_{\text{walks}} K^N \exp[\beta(N_I\epsilon + N_H\epsilon_H)], \tag{3}$$

where N_I are the number of solvent interactions and N_H are the number of hydrogen bonds. The fugacity, which controls the average length of the walk, is denoted by K, and N is the total length of the walk. For convenience we define $\alpha = \epsilon/\epsilon_H$, and without changing the physics of the model, we may set $\epsilon_H = 1$; this simply sets the temperature scale. The partition function then becomes:

$$\mathcal{Z} = \sum_{\text{walks}} K^N \exp[\beta(N_H + N_I\alpha)]. \tag{4}$$

The primary tool we use in this article to map out the phase diagram of this model is the transfer matrix. The transfer matrix method involves studying the model on a lattice strip of length $L_x \to \infty$ and width L_y, finite. In its simplest form, the model is considered on a lattice with periodic boundary conditions in both the x and y lattice directions. In this case the partition function may be rewritten in terms of a matrix product

$$\mathcal{Z} = \text{Tr}\ \mathcal{T}^{L_x}, \tag{5}$$

where $\mathcal{T}$ is the transfer matrix, which contains all the factors required to take account of all possible walk configurations between any two given lattice columns. Details on the transfer matrix method used in this article may be found in Ref. [12].

The partition function may then be expressed in terms of the eigenvalues λ_i of the transfer matrix $\mathcal{T}$:

$$\mathcal{Z} = \sum_i \lambda_i^{L_x}. \tag{6}$$

The dimensionless free energy per spin is given by

$$f = \frac{1}{L_x L_y} \ln \mathcal{Z}. \tag{7}$$

In general the largest eigenvalue is nondegenerate and the sum is dominated by this largest eigenvalue λ_0 giving, in the limit $L_x \to \infty$,

$$f = \frac{1}{L_y} \ln \lambda_0. \tag{8}$$

The problem is now reduced to studying the behavior of the thermodynamic quantities as a function of the width, notably using finite-size scaling techniques. In what follows we will drop the subscript y and denote the lattice width by L. Once the free energy has been calculated, other quantities of interest can be calculated by taking suitable derivatives, for example, the density of the walk on the lattice is given by

$$\rho = \frac{\langle N \rangle}{L_x L_y} = K \frac{\partial f}{\partial K}. \tag{9}$$

It is, however, possible to calculate such quantities directly from the eigenvalues and eigenvectors of the transfer matrix. To see this, it is necessary first to calculate the probability of having a given walk configuration $\mathcal{C}_x$ in column x. This probability is simply the ratio of the partition function restricted to having configuration $\mathcal{C}_x$ in column x and the unrestricted partition function, which in terms of transfer matrices may be written

$$p(\mathcal{C}_x) = \lim_{L_x \to \infty} \frac{\text{Tr}\{T^x |\mathcal{C}_x\rangle\langle\mathcal{C}_x| T^{L_x - x}\}}{\text{Tr}\ T^{L_x}}. \tag{10}$$

Writing $|\mathcal{C}_x\rangle$ in terms of the eigenvectors $|i\rangle$ of $\mathcal{T}$ gives

$$p(\mathcal{C}) = \lim_{L_x \to \infty} \frac{\sum_i \lambda_i^{L_x} \langle i|\mathcal{C}\rangle\langle\mathcal{C}|i\rangle}{\sum_i \lambda_i^{L_x}}, \tag{11}$$

$$p(\mathcal{C}) = \langle 0|\mathcal{C}\rangle^2, \tag{12}$$

where the eigenvectors are normalized. The subscript x may be omitted by invoking translation invariance. The density, for example, is then found using

$$\rho = \sum_{\mathcal{C}} \frac{N(\mathcal{C})}{L} p(\mathcal{C}) = \sum_{\mathcal{C}} \frac{N(\mathcal{C})}{L} \langle 0|\mathcal{C}\rangle^2, \tag{13}$$

where $N(\mathcal{C})$ is the number of occupied lattice bonds in configuration $\mathcal{C}$. The susceptibility can then be calculated either by taking a derivative of the density, or by calculating directly $\langle N^2 \rangle$ for the column, and hence the fluctuation. The two methods give slightly different results for a finite width strip, but agree in the thermodynamic limit. In the present article we choose to calculate the fluctuation directly.

It is straightforward to show that the correlation length ξ depends on the largest two eigenvalues through

$$\xi = \frac{1}{\ln\left(\frac{\lambda_0}{|\lambda_1|}\right)}. \tag{14}$$

If the two eigenvalues become equal in modulus, the correlation length diverges, which is characteristic of the long-range order found at a critical point. For an integer spin model (Ising, XY, Heisenberg, etc.), the transfer matrix is positive (all elements strictly larger than zero) and Frobenius' theorem states that the largest eigenvalue is nondegenerate for finite matrices. This implies that the correlation length may only diverge in the thermodynamic limit $L_x, L_y \to \infty$. In our case, however, the transfer matrix is sparse, and may be block diagonalized into an odd and an even submatrix. The odd submatrix is the transfer matrix for the walks which cross the lattice in the x direction an odd number of times, while the even submatrix is the transfer matrix of walks which cross the lattice an even number of times. We

include in the even submatrix the empty lattice configuration. There is no mathematical reason why the largest eigenvalues of the different submatrices should not coincide, and indeed the lines where this is the case may correspond to transition lines in the phase diagram, since they correspond to lines where the correlation length diverges. It is important to note, however, that the high-density isotropic phase is a critical phase, in which $\xi \to \infty$ everywhere in the infinite lattice system, and so the condition that the two eigenvalues become degenerate is not a foolproof argument, and must be used with care. A standard method for finding phase transition lines in a transfer matrix calculation is to use finite size scaling in the form of Nightingale's renormalization group method [17], which is based on the scale invariance expected close to critical points for large enough lattice sizes. It shows that when solutions exist for the finite-size renormalization equation

$$\frac{\xi_L}{L} = \frac{\xi'_L}{L'}, \tag{15}$$

then these lines are candidate critical transition lines, although, again, such solutions may exist in the high density critical phase without corresponding to transition lines.

The use of transfer matrices in the determination of the phase diagram is convenient, since the partition functions are calculated exactly for infinite strips for any value of the parameters given. Since the partition function is known exactly, there are no convergence problems, and the full phase diagram may be mapped with relatively little effort. The main problem is the size of the matrices, which grow exponentially with the lattice width. This strongly limits the maximal width which may be used, here to $L=9$. Added to the fact that the model contains strong odd and even parity effects, the number of sizes available to more advanced finite-size scaling methods is too small to be of much use. In order to be able to use finite-size scaling to calculate critical exponents for various transition lines, we decided to use a recently introduced implementation of the corner-transfer-matrix renormalization group (CTMRG) method appropriate for lattice walk models [16]. This method, related to the better known density-matrix renormalization group (DMRG) method, enables the calculation of thermodynamic quantities for large lattice sizes, in particular the density of monomers, for lattices with the restriction that $L_x=L_y$. The large lattice sizes are achieved by iteration from smaller lattice sizes. At each iteration the phase space is optimally pruned such that the calculation remains within the constraints of the available computer resources and the error on the quantities of interest is minimized. For further details on the implementation of this model, please see Ref. [10], and references therein.

III. RESULTS

In this section we present the results obtained from the transfer matrix calculations, supplemented when necessary with results from the CTMRG method. We start by studying the small α regime, where the model is expected to behave similar to the pure hydrogen model ($\alpha=0$), studied by Foster and Seno [15] using transfer matrices, and in the Bethe approximation by Buzano and Pretti [11]. At the other end of the scale, when $\alpha=1$ we recover the pure Θ-point model. Considering values of α close to $\alpha=1$ we find new behavior, not present in either the hydrogen model or the Θ-point model. The results found permit the phase diagram to be plotted, and finally we will present results for this phase diagram.

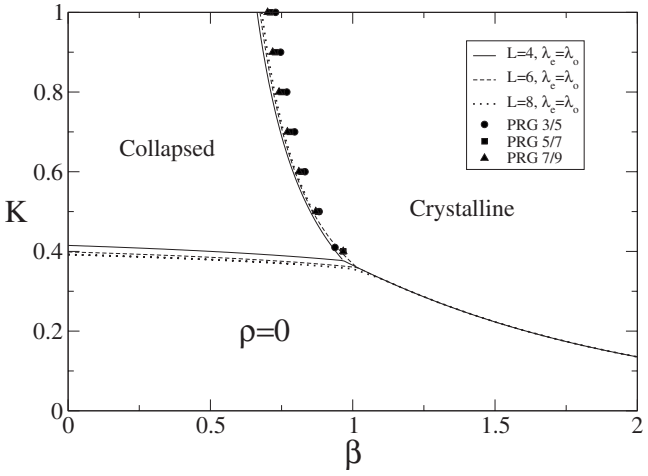

FIG. 4. Phase diagram for $\alpha=0.2$ calculated using eigenvalue crossings (lines), and the phenomenological RG method (points) for the high-ρ transition.

A. Results for $\alpha=0.2$

Foster and Seno [15] studied the model for $\alpha=0$ using transfer matrices. It was shown that the behavior of this model was different from the standard Θ-point model. The collapse transition was now first order, corresponding to a jump in the density as the low-K transition line is followed. The model also presents a high-K transition line separating the usual isotropic dense (liquid) phase from an anisotropic (crystalline) phase. They gave evidence that this transition was critical, in contradiction to extended mean-field type calculations performed by Buzano and Pretti [11] on the same model, which predicts a first order transition.

In this section we show that for $\alpha=0.2$ we recover a similar behavior, showing that the crystalline phase and its associated phase transitions persist over a range of values of α. Transfer matrix calculations are combined with those of the CTMRG method to obtain more accurate results for the critical behavior of the liquid-crystalline transition, which we confirm to be of second order.

The phase diagram for $\alpha=0.2$ is shown in Fig. 4, calculated using transfer matrices. In Fig. 4 the low-K transition line between the finite-length $\rho=0$ phase and the dense phases is found by setting the largest eigenvalue of the transfer matrix to 1. When even lattice sizes are considered, the largest eigenvalue corresponds to the largest eigenvalue from the odd sector of the transfer matrix (λ_o) for small β and the largest eigenvalue of the even sector (λ_e) when β is large. The point where the two cross, $\lambda_e=\lambda_o$, is identified as the

crystallization transition. This line extends both into the high and low density phases. In the low density phase the line corresponds to the crossing of subdominant eigenvalues (since the largest eigenvalue, corresponding to the empty lattice, is $\lambda_0=1$). This may be identified with a disorder line, indicating a change of local order. In the dense phase, however, the crossing corresponds to a crossing of the two largest eigenvalues, which from Eq. (14) may be seen to correspond to a divergent correlation length. This line may then be identified with a special critical line where the long-range order changes. The identification of this line with the phase boundary between the liquid and crystalline phases is not straightforward since the liquid phase is a critical phase, so it is possible that the line is buried within this phase. To verify that this is indeed the transition line, we compare the results with results calculated from Nightingale renormalization group arguments (the points shown also in Fig. 4). In Fig. 8 we give finite-size estimates for the transition line for $\alpha=0.2$, $K=2$, showing the coherence of the different methods, and verifying that the eigenvalues cross at the transition.

Transfer matrices are limited by the maximal lattice width that may be obtained, which in turn limits the number of lattice sizes which may be used for studying finite-size behavior. For this reason we turn to the CTMRG method, which produces results for large lattice sizes, permitting better estimates of the critical exponent, critical density, and temperature. Unlike the transfer matrix method, where we dealt with infinite strips of finite width, in what follows we will be looking at a lattice finite in both directions, with $L_x=L_y=L$.

In order to use finite-size scaling, we consider the scaling form for the density. Here it was convenient to fix K and vary β, for which we expect the following scaling form:

$$\rho_L(\beta)=\rho_\infty(\beta)+L^{1/\nu-2}\tilde{\rho}(|\beta-\beta_c|L^{1/\nu}). \tag{16}$$

The scaling form given in Eq. (16) gives the leading behavior close to the critical point. The corrections to scaling may be expected to be negligible "close enough" to the critical point. It is clear that if the following variables are plotted:

$$x=|\beta-\beta_c|L^{1/\nu}, \tag{17}$$

$$y=[\rho_L(\beta)-\rho_\infty]L^{2-1/\nu}, \tag{18}$$

then, close enough to the critical point, the points plotted should fall onto the universal curve $y=\tilde{\rho}(x)$. This phenomenon is known as data collapse. The values of β_c, ν, and ρ_∞ are not known, but can be determined by choosing values which give the best data collapse. It is of course useful to know some estimate of β_c and ρ_∞ by some other method, estimates which we are able to improve by optimizing the collapse of data close to the transition. In Fig. 5 we plot the density as a function of β for $K=2$ and a lattice $L=1000$. It is readily seen that $\rho_\infty\approx 0.99$ and $\beta_c\approx 0.62-0.63$. Starting with these initial values we determined values of the parameters which gave the best data collapse, and we find $\rho_\infty=0.989\pm 0.001$, $\beta_c=0.6222\pm 0.0005$, and $\nu=0.87\pm 0.02$. The resulting curve $y=\tilde{\rho}(x)$ is shown in Fig. 6. The error bars correspond to the range of values over which the parameters may be varied before we clearly no longer have collapse of the data. We limited the lattice sizes to $L\leq 160$ in the study, since, due to the factor $L^{1/\nu}$ in the variable x, the points which appear in the figure are closer to the critical temperature as the lattice size increases. The error in the determination of the point is also amplified by the factor $L^{2-1/\nu}$ in y. These considerations limit the maximum size considered.

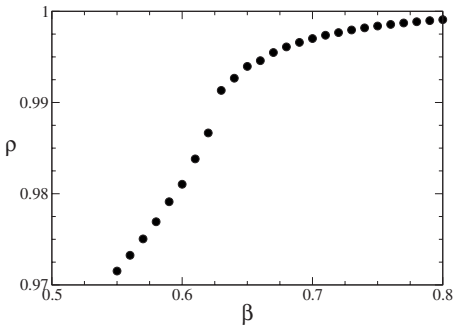

FIG. 5. Density calculated for $\alpha=0.2$, $K=2$ using CTMRG with $L=1000$

Clearly, in the crystalline phase, the walk will wish to align with one of the lattice directions, with a tendency to eject corners from the bulk. While we expect the density of corners to differ in the two phases, we note that the data collapse indicates that the density of the walk has not reached one, and so the density of corners must be nonzero. This means that while the fluctuations in the numbers of corners should diverge at the transition, the corner density is not a good order parameter. On the other hand the crystalline phase is anisotropic, while the two other phases are isotropic. A natural order parameter is then $\delta\rho=|\rho_v-\rho_h|$, the difference between the densities of vertical and horizontal bonds. In the isotropic phases this will vanish, but not in the anisotropic phase. We are not able to calculate this quantity with our CTMRG calculation, since the symmetries of the lattice are explicitly used in the method [16] but we have direct access to this parameter using transfer matrices through

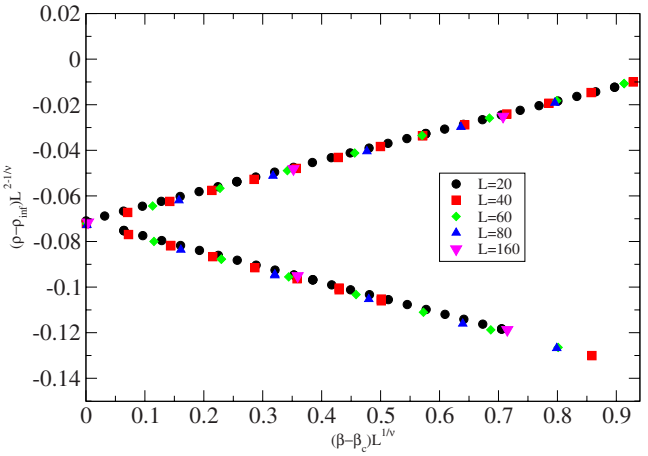

FIG. 6. (Color online) Data collapse for the density close to the transition using data from the CTMRG method with $\alpha=0.2$, $K=2$. The finite-size scaling form of the density is taken with $\rho_\infty=0.989$, $\beta_c=0.6222$, and $\nu=0.87$

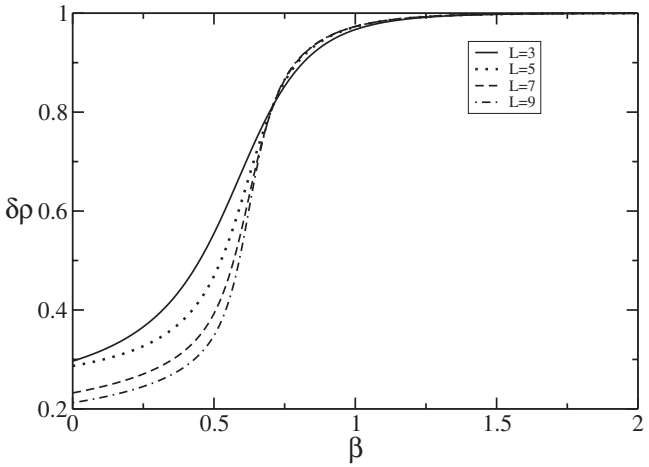

FIG. 7. Plot of $\delta\rho=|\rho_h-\rho_v|$ for $\alpha=0.2$ and $K=2$.

$$\delta\rho = \frac{1}{L}\sum_{\mathcal{C}} |N_v(\mathcal{C}) - N_h(\mathcal{C})|p(\mathcal{C}). \tag{19}$$

This is shown in Fig. 7 for $\alpha=0.2$, $K=2$. The peaks of the fluctuations in $\delta\rho$ and the density of corners ρ_c may be used as estimators for the liquid-crystal phase transition line. These are shown, along with other estimates, in Fig. 8.

B. Results for $\alpha=0.8$

In this section we choose to study the phase diagram for $\alpha=0.8$, where the model is found to have a very different behavior. The phase diagram calculated using the phenomenological renormalization group is shown in Fig. 9. While we still find the three phases: the low-K zero density phase, and the liquid and crystalline phases at higher K, the diagram is quite different in appearance.

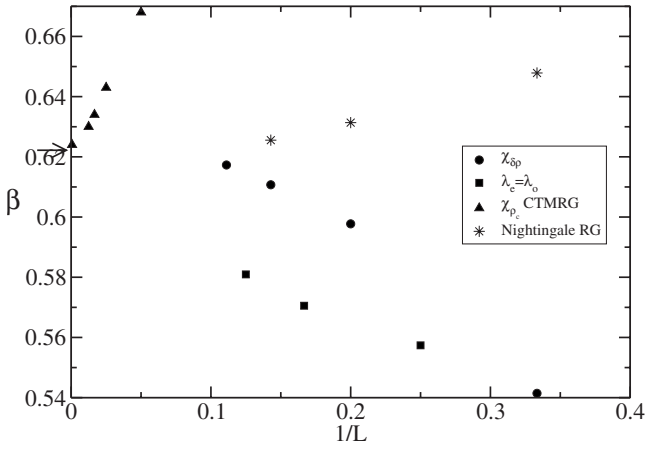

FIG. 8. Estimates for β_c using various methods for $\alpha=0.2$ and $K=2$. Arrow shows the value found using the data collapse method $\beta_c=0.6222$. ● represent the peaks of the fluctuations of $\delta\rho$, while the triangles correspond to the position of the peaks of the fluctuations in the corner density, calculated with CTMRG. ∗ gives the position of the solutions to the Nightingale RG method, and the squares the position estimated using the condition that $\lambda_e=\lambda_o$.

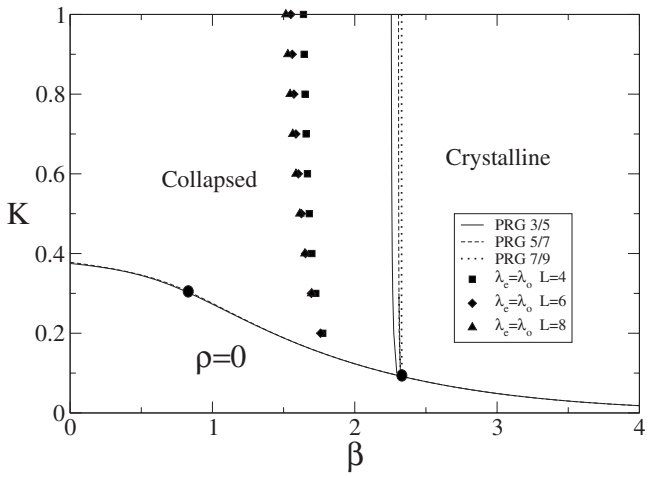

FIG. 9. Phase diagram for $\alpha=0.8$ calculated using Nightingale's phenomenological RG method. The special transitions along the low-K line are shown. The first is the θ point for $\alpha=0.8$ while the second is the collapsed-crystalline transition. The solution of the condition $\lambda_e=\lambda_o$ is shown for various sizes using points, and can be seen to give a distinct line, which does not converge to the collapsed-crystalline transition line.

As the low-K transition line is followed, we have first a Θ-type transition, followed later by a crystallization transition. The transition from finite walk to the dense phases is a second order transition in the self-avoiding walk class for $\beta<\beta_\Theta$ becoming first order for $\beta>\beta_\Theta$. In Fig. 10, the corner density fluctuations are plotted along the low-K transition line. The corner susceptibility is calculated by introducing an additional parameter corresponding to a bending energy, and then applying the fluctuation dissipation theorem. Defining $\beta_{\text{corn}}=\epsilon_{\text{corn}}/kT$, we define

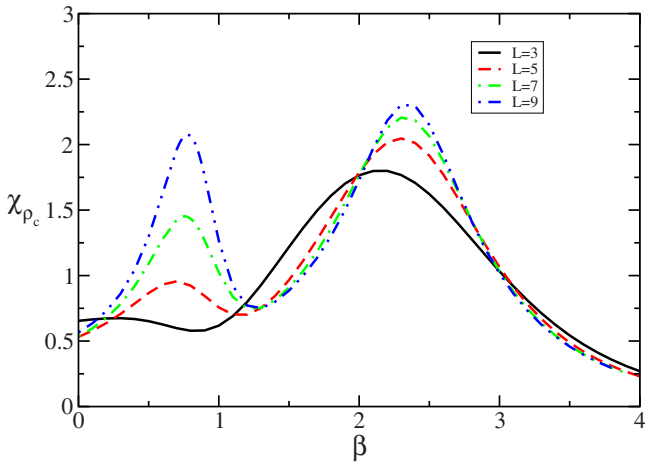

FIG. 10. (Color online) Fluctuations of the number of corners in the walk for $\alpha=0.8$ calculated along the lower critical line showing clearly the existence of two transitions. Both transitions appear to be critical.

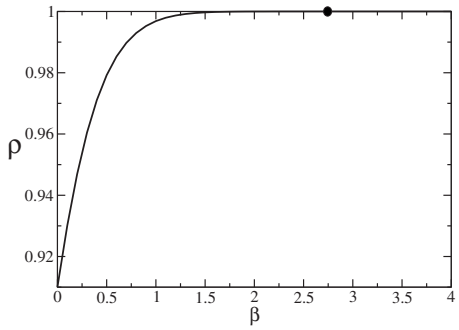

FIG. 11. Bond density calculated for $K=2$, $\alpha=0.8$ using CTMRG with $L=1000$. The circle indicates the location of the collapsed-crystalline phase transition calculated using data collapse (see Fig. 12). The transition can be seen to occur at a density $\rho=1$.

$$\chi_c = \frac{\partial \rho_c}{\partial \beta_{\text{corn}}}. \tag{20}$$

The formation of two peaks may clearly be seen, corresponding to the two special points along the low-K line. Interestingly, unlike the $\alpha=0.2$ case, the two transitions appear to be critical.

We now investigate the nature of the transition line between the two dense phases. What is interesting is that the condition $\lambda_e=\lambda_o$ for even transfer matrices, which coincided with this line for $\alpha=0.2$, is well within the isotropic collapsed phase here. This is not contradictory, since the collapsed phase is critical, and so the condition $\lambda_e=\lambda_o$ must correspond to a change of order within the critical phase, but not to the phase boundary. This is the first indication that the transition line here is different from the transition in the previous section. Here again we turn to CTMRG and look for the conditions for data collapse. The density ρ appears to have saturated to 1 (see Fig. 11), making it impractical to use, however, it is expected that the density of corners ρ_c should scale in the same way, and this is what we use here. The best fit was obtained for $\rho_{c,\infty}=0.2744\pm0.0005$, $\beta_c=2.349\pm0.003$, and $\nu=0.96\pm0.02$, and is shown in Fig. 12. In Fig. 13 we show different estimates for the critical point for $K=2$ and $\alpha=0.8$.

C. The $\alpha-\beta$ phase diagram

The full phase diagram is expressed in three variables K, α, and β, and is difficult to picture. In this section we present the phase diagram in the α-β plane calculated on the surface $K=K^*$, where K^* is the value of K required for the average length of the walk to just diverge. This is what is generally calculated in Monte Carlo simulations, and corresponds to the "long polymer in dilute solution" limit.

When $\alpha=1$ the model corresponds to the pure Θ-point model, with only one transition point on the $K=K^*(\beta)$ line; the Θ tricritical point. This point is easily found by looking at the crossings of the finite-size estimates of ν calculated along the line of solutions to Eq. (14). For small β these estimates tend to $\nu_{\text{SAW}}=3/4$ while for large β they tend to

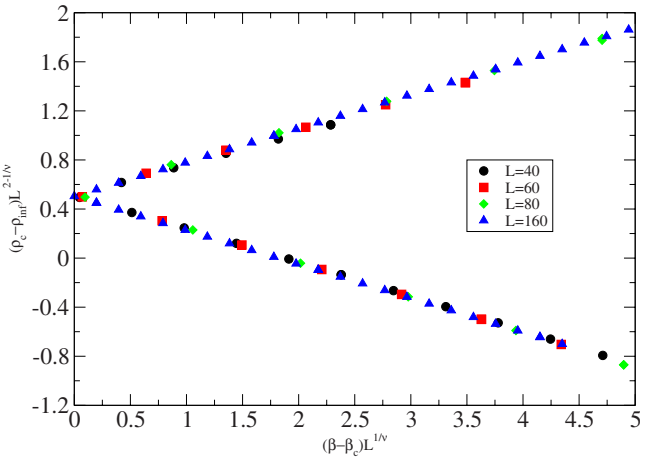

FIG. 12. (Color online) Data collapse of the corner density ρ_c for $\alpha=0.8$, $K=2$ fitted with $\rho_{c,\infty}=0.2744$, $\beta_c=2.349$, and $\nu=0.96$.

$\nu=1/2$, characteristic of the first order collapsed-walk line in two dimensions. In between these two behaviors we find a point, which tends to $\nu_\Theta=4/7$. By the way the estimates tend to their limiting values, this intermediate point shows up as a crossing in the different finite-size estimates. Looking at these estimates as a function of α leads to the extended line of tricritical points in the Θ-point universality class. This is the usual method for determining the location of the tricritical point, but it requires the use of three lattice widths to determine one estimate. Here we propose a different method. The low-K transition line is determined by looking for solutions of the phenomenological renormalization group (RG) Eq. (15) with the correlation length defined by Eq. (14) taking $\lambda_0=1$ and λ_1 is the largest eigenvalue taken from the odd or even sectors of the transfer matrix. A tricritical point has an additional correlation length which diverges, corresponding to the two relevant directions in the renormalization group sense. We look for the solutions of Eq. (15) with a correlation length calculated using the largest eigenvalue from the odd and even sectors. This method only requires

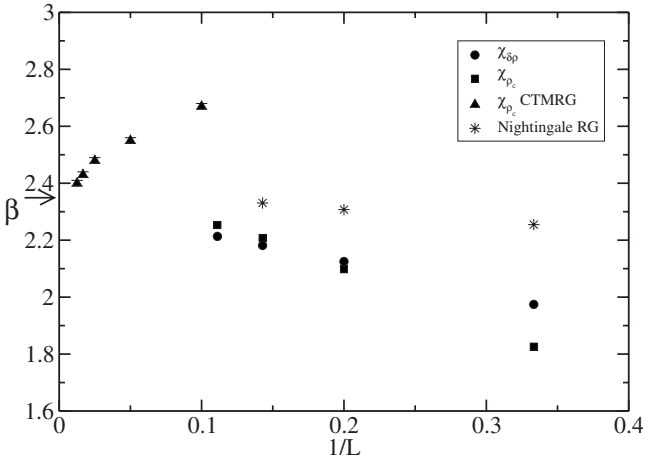

FIG. 13. Estimates for β_c using various methods for $\alpha=0.8$, $K=2$. The arrow shows the value $\beta_c=2.349$ found using the data collapse method.

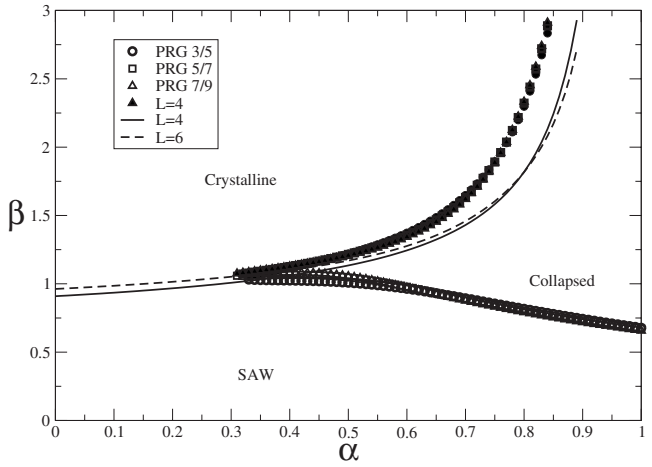

FIG. 14. Phase diagram in the α-β plane calculated using phenomenological RG and eigenvalue crossings. The solid lines show the solutions to the condition $\lambda_e=\lambda_o$, expected to coincide with the self-avoiding walk-crystalline transition.

two lattice widths to estimate the location of the tricritical point. Additionally, the high-K transition line is found using Eq. (15) with these same two eigenvalues. The method described therefore also locates the position of the crystallization transition along the low-K transition line. The phase diagram calculated by this method is shown in Fig. 14. For small α there is no solution. However this region of the phase diagram corresponds to the region which is expected to behave similarly to the pure hydrogen-bonding model, and therefore the condition $\lambda_e=\lambda_o$ corresponds to the first order transition line.

In Fig. 15 the phase diagram is calculated using the peaks of the two susceptibilities. The upper line is calculated by looking for the peak of the fluctuations of $\delta\rho$ while the lower line is calculated using the peaks of the fluctuations of ρ. For α less than about 0.4 the two sets of lines merge and give estimates for the single hydrogen-bonding-like first order line, while for values of α larger than about 0.5 the two sets of lines are distinct, the lower line corresponding to the line of Θ-like tricritical points, while the upper line corresponds to the critical crystallization line. Somewhere in the region $\alpha=0.4\rightarrow0.5$ these two lines merge into a higher order multicritical point.

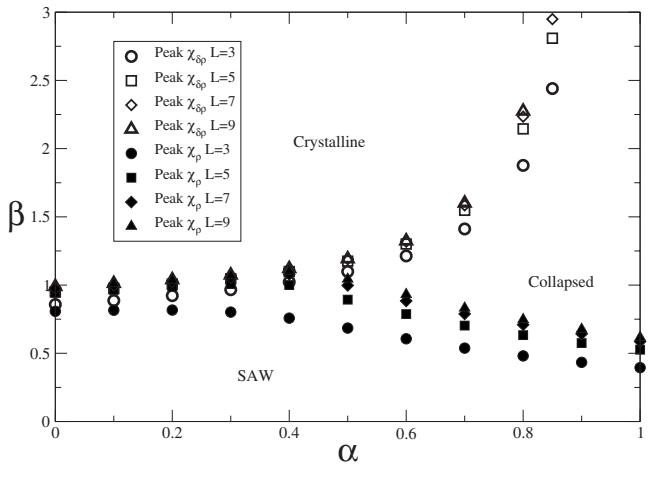

FIG. 15. Phase diagram in the α-β plane calculated using the peaks of χ_ρ and $\chi_{\delta\rho}$ calculated using transfer matrices. The peaks of ρ fluctuations pick out the line of Θ points, while the peak of $\delta\rho$ fluctuations pick out the transition between the isotropic collapsed phase and the anisotropic crystalline phase. These two lines merge to form the first order transition line separating the SAW phase from the crystalline phase.

Looking closely at Fig. 14 it may be seen that the upper and lower transition lines tend to come together in the region $\alpha=0.3\rightarrow0.5$, with the lower line developing a plateau. It is probable that the multicritical point is not located at the cusp where solutions end, but at a higher value of α, probably in the same range of values. The methods employed in this article were not able to determine this point more accurately. The CTMRG, which enables larger sizes to be obtained, becomes impractical in this region, particularly when the number of constraints required to define the point is considered.

IV. DISCUSSION

There are now a number of similar models which display an anisotropic crystalline phase, with a variety of different types of high-density transition. The first is the vertex-interacting self-avoiding walk due to Blöte and Nienhuis [7], which displays an Ising-like high-density transition with $\nu=1$. The hydrogen-bonding model was shown to also have a critical transition [15], but in a different universality class, which is confirmed in this article, where the value $\nu\approx0.87$ is found. Lastly the bond-interacting Θ-point model [12] which is conjectured to have a softer, higher order critical transition.

What is interesting in the model presented here is that two different high-K critical behaviors are displayed in one model. For smaller values of α the transition from the collapsed to crystalline phase is of the hydrogen-bonding class, and occurs at densities which are close to $\rho=1$ but on close inspection we clearly have $\rho<1$, as may be seen in Fig. 5.

Data collapse for $\alpha=0.8$ gave $\nu=0.96$ for the best fit, however, the fitting was less clear than for $\alpha=0.2$ and it is possible that the correction terms are more important. The value of ν calculated would then be an effective exponent. It is tempting to conjecture that the true value of $\nu=1$, in analogy with the vertex-interacting model. However, as may be seen in Fig. 11 the transition may be seen to occur well after the density saturates to $\rho=1$. If this is the case, then the walk is essentially a Hamiltonian walk at the transition, and looks very similar to the model with a penalty for the formation of corners in the Hamiltonian walk limit studied by Saleur [18], where he conjectured that the transition was of infinite order BKT transition of the same type as in the F model, but is in contradiction to the results presented here. This contradiction was first seen in the hydrogen model in the Hamiltonian limit [15], where the transfer matrix results also gave estimates close to $\nu=1$. This is a point which warrants further investigation.

The results found here are to some extent confirmed by a Monte Carlo study, mainly in three dimensions, which has appeared during the final stages of this work [19]. Notably, based on a flat-PERM study, a similar phase transition to that presented in Figs. 14 and 15 is found. The transition from the collapsed phase to the crystalline phase along the surface where the walk length just diverges was seen to be probably critical, as is the case here.

[1] P. G. de Gennes, *Scaling Concepts in Polymer Physics* (Cornell University Press, Ithaca, 1979).
[2] J. des Cloiseaux and G. Jannink, *Polymers in Solution: Their Modelling and Structure* (Oxford University Press, Oxford, 1990).
[3] Carlo Vanderzande, *Lattice Models of Polymers* (Cambridge University Press, Cambridge, 1998).
[4] C. Domb, Polymer **15**, 259 (1974).
[5] F. T. Wall and J. Mazur, Ann. N. Y. Acad. Sci. **89**, 608 (1961).
[6] P. G. de Gennes, Phys. Lett. **38A**, 339 (1972).
[7] H. W. J. Blöte and B. Nienhuis, J. Phys. A **22**, 1415 (1989).
[8] W. Guo, H. W. J. Blöte, and B. Nienhuis, Int. J. Mod. Phys. C **10**, 301 (1999).
[9] S. O. Warnaar, M. T. Batchelor, and B. Nienhuis, J. Phys. A **25**, 3077 (1992).
[10] D. P. Foster and C. Pinettes, J. Phys. A **36**,10279 (2003).
[11] C. Buzano and M. Pretti, J. Chem. Phys. **117**, 10360 (2002).
[12] D. P. Foster, J. Phys. A: Math. Theor. **40**, 1963 (2007).
[13] F. Jürgen Stilck, Kleber D. Machado, and Pablo Serra, Phys. Rev. Lett. **76**, 2734 (1996).
[14] J. Bascle, T. Garel, and H. Orland, J. Phys. II **3**, 245 (1993).
[15] D. P. Foster and F. Seno, J. Phys. A **34**, 9939 (2001).
[16] D. P. Foster and C. Pinettes, Phys. Rev. E **67**, 045105 (2003).
[17] M. P. Nightingale, Physica A **83**, 561 (1975).
[18] H. Saleur, J. Phys. A **19**, 2409 (1986).
[19] J. Krawczyk, A. L. Owczarek, and T. Prellberg, J. Stat. Mech.: Theory Exp. 2007, P09016 (2007).